CAV2021
11th International Symposium on Cavitation
May 10-13, 2021, Daejon, Korea

The effect of nuclei on the attachment hysteresis in cavitating trailing vortices

James A. Venning[1]*, Rhys A. Paul[1], Matthew T. Khoo[1,2], Bryce W. Pearce[1] and Paul A. Brandner[1]

[1]Cavitation Research Laboratory, University of Tasmania, Launceston, Tasmania, Australia
[2]Maritime Division, Defence Science and Technology Group, Melbourne, Victoria, Australia

Abstract: The incidence hysteresis between the attachment and detachment angles of a trailing vortex cavity behind an elliptical hydrofoil is investigated for two nuclei populations in a cavitation tunnel. Deplete and dense population were realized through natural and artificially seeded nuclei, respectively. The cavitation appearance was monitored for a range of incidences, and two hysteretic behaviours were observed. In a nuclei-deplete flow, the temporal delay required to ingest and activate a susceptible nucleus and associated additional tension caused a larger incidence for cavity attachment. With dense seeding, however, the continual supply of nuclei into the cavity sustained the attached cavity at much lower incidences.

Keywords: Cavitation; vortex cavitation; TVC; nuclei.

1. Introduction

Cavitation about marine propulsors or in turbomachinery often occurs first in vortical flows. Vortices cause high rotational velocities and associated low pressures. The deleterious effects of cavitation include unsteady loading, vibration, noise, inefficiencies, and increased visual signatures. While pure water may withstand extremely high tensions [1], impurities such as microbubbles, microorganisms, or solid particles provide nucleation sites, allowing cavitation at higher pressures.

Since cavitation is invariably heterogeneous in practical hydrodynamic contexts, the cavitation performance in an experiment is inextricably linked to the nuclei content[2, 3]. Cavitation inception in deplete flows is highly variable [4], and Boulon et al. [5] noted that the first appearance of cavitation does not

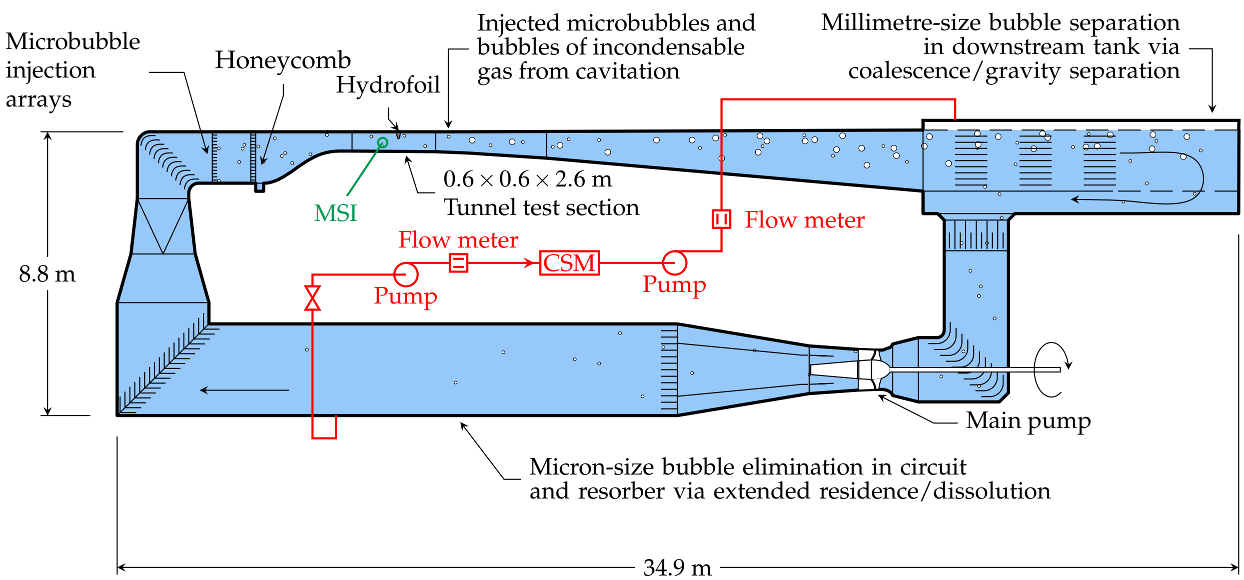

Figure 1. Schematic of the cavitation tunnel showing circuit architecture and ancillaries for microbubble control and CSM circuit integration (red). The location for the optical MSI measurement is given in green.

*Corresponding Author: James Venning, james.venning@utas.edu.au

provide a reliable criterion for TVC inception. As such, the desinent cavitation number is often reported as the critical cavitation parameter [6]. However, once a cavity has attached to the hydrofoil, it may remain at higher pressures than the vapour pressure [7] due to local supersaturation of the flow and gaseous diffusion into the cavity. In the present study, we investigate this cavitation hysteresis for two nuclei populations. Two nuclei contents are achieved through the injection of an abundant microbubble population into a nuclei-deplete flow COPY FROM ABSTRACT. We report on the incidence at which the trailing cavity attaches onto the hydrofoil, and the angle at which the cavity detaches, and show these to be strongly dependent on the nuclei population.

2. Setup

Experiments were performed at the Cavitation Research Laboratory at the University of Tasmania, Australia. An elliptical planform hydrofoil was installed in the test-section ceiling, 1.45 m downstream of the test-section entrance, see figure 1. A stainless-steel hydrofoil with a NACA 0012 profile had a chord, c, of 150.0 mm and a span of 176.7 mm, giving an aspect ratio of 3.0.

Microbubbles were generated via the depressurisation of super-saturated water through an array of 0.5 mm orifices and injected upstream of the contraction [8]. The diameters of these microbubbles were measured in the test section with Mie-scattering Imaging (MSI). The microbubbles were illuminated with a 532 nm laser (Ekspla, Lithuania) and defocused photographs were acquired with a 48 megapixel camera (IO Industries, Canada). The spatial frequency of the defocussed images is dependent on the diameter of the bubble [9, 8]. The cumulative concentration, C, of the bubble population is given in figure 2 as a function of the critical tension, T. The abundant population (green) sustains essentially no tension, and as such will activate at pressures near vapour pressure. Whereas the deplete population requires significant tensions for activation.

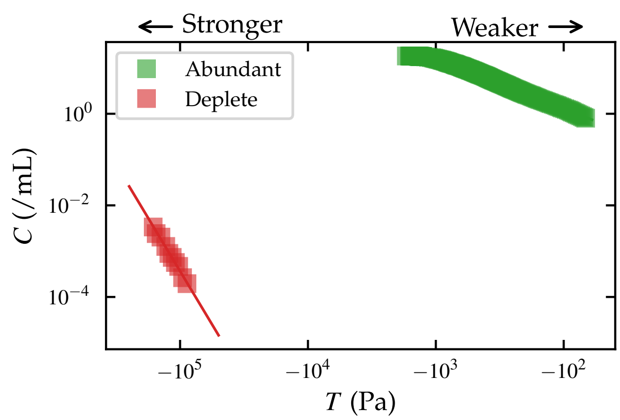

Figure 2. Measurements of the two nuclei populations considered in this experiment. The populations are presented as cumulative distributions (C) counted from largest (weakest) to smallest (strongest). The generated (abundant) population was measured with MSI and the natural (deplete) population was measured with a CSM.

To measure the natural nuclei population, which is constant around the circuit [10], mechanical activation is required due to the small diameter and low concentration of this population. Water was sampled from the lower leg of the tunnel and passed through a cavitation susceptibility meter (CSM), see figure 1, where the natural nuclei population is mechanically activated and acoustically counted, as detailed in Venning et al. [11]. This population is far stronger than the generated population in that it has very few weak nuclei, and as such is termed 'deplete' in this paper. The dissolved oxygen was maintained below 3.3 mg/L.

The cavitation performance of the hydrofoil was measured by setting the cavitation number (σ) and the Reynolds number (Re) via the static pressure (p_∞) and freestream velocity (U_∞):

$$\sigma = \frac{p_\infty - p_\text{v}}{{}^1\!/_2 \rho U_\infty^2}, \qquad Re = \frac{U_\infty c}{\nu}, \tag{1}$$

*Corresponding Author: James Venning, james.venning@utas.edu.au

where p_v is the vapour pressure, ρ is the density, and ν is the kinematic viscosity of the water. The Reynolds number was fixed at 1.25×10^6. From a single-phase incidence, the angle was then increased continuously at a rate of $0.127° \, s^{-1}$ until the cavity attached to the hydrofoil, and the incidence was recorded. The angle was then decreased until the cavity detached from the hydrofoil and the incidence was recorded.

3. Results

The typical appearance of two states of a cavitating vortex (attached and detached) are shown in figure 3. The detached case (left) is at a lower incidence where the hydrofoil generates insufficient tension for the cavity to attach to the hydrofoil surface. In the attached case (right), slightly more tension is applied by increasing the incidence, and the cavity now attaches to the surface. In this instance, it combines with a small leading-edge sheet cavity.

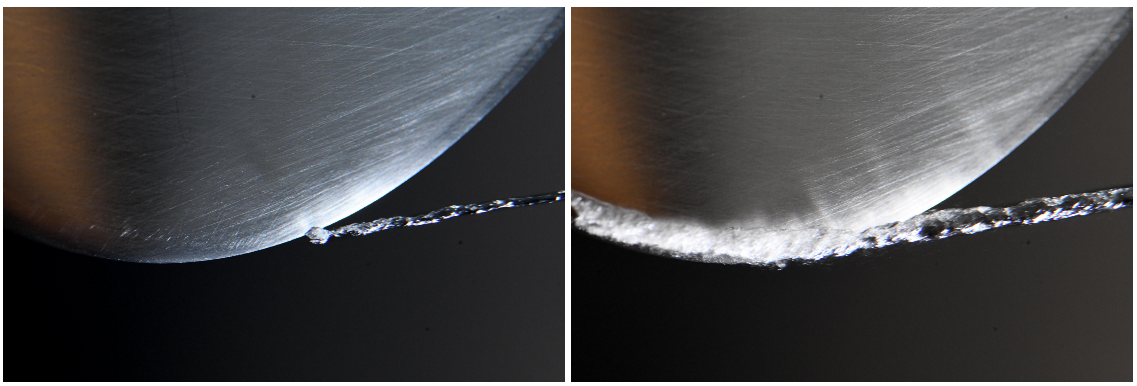

Figure 3. Comparison showing detached (left) and attached (right) trailing vortex cavitation.

The attachment and detachment angles are presented in figure 4 for each seeding configuration and for a range of cavitation numbers. For each cavitation number tested, both attachment and detachment were observed, and this pair is presented with a vertical line between the two points, representing the attachment hysteresis.

Two distinct hysteretic behaviours were observed in the trailing vortex cavitation. When the flow is deplete of nuclei, a much higher tension is necessary to form any cavitation (i.e. the water sustains some tension before rupturing). Cavitation inception is delayed while waiting for the arrival of a sufficiently weak nucleus due to the sparse and stochastic nature of the deplete population. As the tests were performed by continuously increasing the incidence (including during this delay), the attachment incidence is high. In many cases, cavitation does not occur until the tension is sufficient to attach the cavity immediately to the hydrofoil tip. When the angle of incidence is reduced, thereby reducing the tension, the cavity is sustained to a lower incidence than the attachment angle.

The other form of hysteresis observed is driven by different physics and occurs only with the densely seeded flow. Here, the nuclei are attracted inward in the trailing vortex if the buoyancy force overcomes the Stokes drag. These nuclei grow in the low-pressure region. Due to their abundance, the nuclei form a contiguous cavity, with large numbers coalescing into the cavity along its length. The cavity attaches to the hydrofoil with sufficient tension. When the tension is subsequently reduced, the constant supply of nuclei near the tip continually feed gas into the cavity, sustaining the trailing vortex cavity to much lower tensions.

4. Conclusions

Measurements of hydrofoil trailing-vortex cavitation have been presented for two different nuclei populations. The attachment and detachment angles show a hysteretic behaviour, however, the behaviour is different according to the seeding. With no additional nuclei, a temporal delay due to long nucleus arrival time causes one hysteretic behaviour. With seeding, coalescence and gas diffusion into the vortex cavity sustain the cavity to lower incidences.

*Corresponding Author: James Venning, james.venning@utas.edu.au

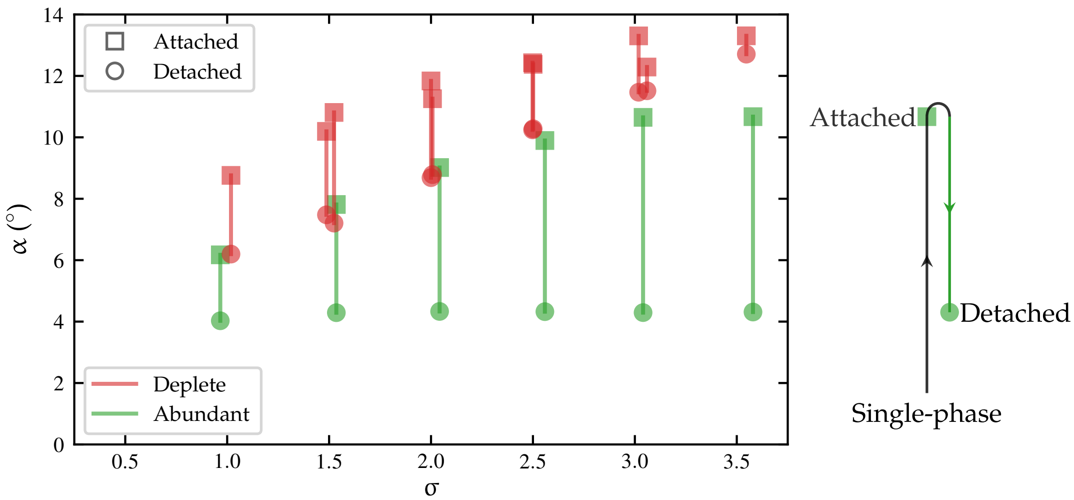

Figure 4. Incidence hysteresis of the cavity attachment for different seeding configurations. The incidence at cavity attachment is indicated by the square at the top of each vertical line, and the detachment angle by the circle at the bottom. The right-hand side shows the typical experimental procedure. The experiment starts in a single-phase condition. The incidence is increased until cavity attachment, then decreased until cavity detachment.

References

1. Lyman J Briggs. Limiting negative pressure of water. *Journal of Applied Physics*, 21(7):721–722, 1950.
2. Joseph Katz and Allan Acosta. Observations of nuclei in cavitating flows. In *Mechanics and Physics of Bubbles in Liquids*, pages 123–132. Springer, 1982.
3. Roger EA Arndt and Brant H Maines. Nucleation and bubble dynamics in vortical flows. *Journal of Fluids Engineering*, 122(3):488–493, 2000.
4. M T Khoo, J A Venning, B W Pearce, and P A Brandner. Statistical aspects of tip vortex cavitation inception and desinence in a nuclei deplete flow. *Experiments in Fluids*, 61, 2020. ISSN 1432-1114. doi: 10.1007/s00348-020-02967-x.
5. O. Boulon, J.-P. Franc, and J.-M. Michel. Tip Vortex Cavitation on an Oscillating Hydrofoil. *Journal of Fluids Engineering*, 119(4):752–758, 1997. ISSN 00982202. doi: 10.1115/1.2819494.
6. Robert W. Kermeen. Water tunnel tests of NACA 4412 and Walchner profile 7 hydrofoils in noncavitating and cavitating flows. Technical Report 47-5, Pasadena, California, 1956.
7. Ali Amini, Martino Reclari, Takeshi Sano, Masamichi Iino, Matthieu Dreyer, and Mohamed Farhat. On the physical mechanism of tip vortex cavitation hysteresis. *Experiments in Fluids*, 60(7):118, 2019.
8. Patrick S. Russell, Luka Barbaca, James A. Venning, Bryce W. Pearce, and Paul A. Brandner. Measurement of nuclei seeding in hydrodynamic test facilities. *Experiments in Fluids*, 61(79), 2020. ISSN 14321114. doi: 10.1007/s00348-020-2911-2.
9. Patrick Russell, James Venning, Bryce W. Pearce, and Paul A. Brandner. Calibration of Mie scattering imaging for microbubble measurement in hydrodynamic test facilities. *Experiments in Fluids*, 61(93), 2020. ISSN 14321114. doi: 10.1007/s00348-020-2927-7.
10. M. T. Khoo, J. A. Venning, B. W. Pearce, K. Takahashi, T. Mori, and P. A. Brandner. Natural nuclei population dynamics in cavitation tunnels. *Experiments in Fluids*, 61(34), 2020. ISSN 14321114. doi: 10.1007/s00348-019-2843-x.
11. J.A. Venning, M.T. Khoo, B.W. Pearce, and P.A. Brandner. Background nuclei measurements and implications for cavitation inception in hydrodynamic test facilities. *Experiments in Fluids*, 59(4), 2018. ISSN 07234864. doi: 10.1007/s00348-018-2520-5.

*Corresponding Author: James Venning, james.venning@utas.edu.au